Orientational transitions in a nematic liquid crystal confined by competing surfaces

I. Rodríguez-Ponce,* J. M. Romero-Enrique, and L. F. Rull
Departamento de Física Atómica, Molecular y Nuclear, Area de Física Teórica, Universidad de Sevilla, Apartado 1065, E-41080 Sevilla, Spain

(Received 11 January 2001; published 17 October 2001)

The effect of confinement on the orientational structure of a nematic liquid crystal model has been investigated by using a version of density-functional theory. We have focused on the case of a nematic confined by opposing flat surfaces, in slab geometry (slit pore), which favor planar molecular alignment (parallel to the surface) and homeotropic alignment (perpendicular to the surface), respectively. The spatial dependence of the tilt angle of the director with respect to the surface normal has been studied, as well as the tensorial order parameter describing the molecular order around the director. For a pore of given width, we find that, for weak surface fields, the alignment of the nematic director is perpendicular to the surface in a region next to the surface favoring homeotropic alignment, and parallel along the rest of the pore, with a sharp interface separating these regions (S phase). For strong surface fields, the director is distorted uniformly, the tilt angle exhibiting a linear dependence on the distance normal to the surface (L phase). Our calculations reveal the existence of a first-order transition between the two director configurations, which is driven by changes in the surface field strength, and also by changes in the pore width. In the latter case the transition occurs, for a given surface field, between the S phase for narrow pores and the L phase for wider pores. A link between the L-S transition and the anchoring transition observed for the semi-infinite case is proposed.

DOI: 10.1103/PhysRevE.64.051704 PACS number(s): 61.30.Hn, 61.30.Cz, 61.30.Pq

I. INTRODUCTION

In recent years there has been a vast theoretical effort to understand the properties of liquid crystals in bulk phases. However, it is only recently that the interfacial phenomena presented by these complex fluids have attracted increasing interest. The ability to manipulate the direction of the preferred molecular alignment, the *director*, by coupling to surfaces, is a property with great practical interest. For this reason, there is now an effort at trying to describe this rich *surface phenomenology* in liquid crystals. These studies have mainly used phenomenological Landau–de Gennes approaches and aimed to describe, with more or less success, different phenomena such as subsurface deformations [1–3] (ordering close to a surface), changes in the alignment of the director due to the interaction with a solid substrate [4], the nematic-isotropic transition [5], wetting [6], etc. On the other hand, microscopic-type theories claim to provide a more precise description of these inhomogeneous problems since they take account of the structure at the molecular scale. In this framework, there is a recent literature describing attemps to answer such questions and it is supposed to provide more satisfactory theories on the interfacial phenomena. For example, by employing an Onsager-type theory van Roij *et al.* [7] investigated the problem of biaxiality and wetting for the Zwanzig model. Teixeira discussed in a recent work [8] the existence of subsurface deformations for the case of a confined nematic phase by using a generalized van der Waals theory. In previous papers, also employing this last approach, we studied surface phenomena in the case of a nematic in contact with a single wall [9] as well as capillary effects in the case of a nematic in slab geometry with symmetric walls [10]. In Ref. [9] our attention was restricted to the study of a nematic in the presence of a solid interface. Model parameters were chosen such that the surface forced the molecules to lie perpendicular to the interface (homeotropic orientation) while in the nematic-isotropic interface the nematic director had a preference for lying parallel to the interface (planar orientation). In the model, surface parameters responsible for the order are the particle-wall interaction (ϵ_W) and the particle-particle interaction (ϵ_C) which plays an important role in the interplay between anchoring and wetting transitions. A first-order anchoring transition between planar and homeotropic regimes was found; in a μ-T (chemical potential–temperature) representation (see Fig. 1) this transition appears as a line called the anchoring line. This line approaches the nematic-isotropic transition line tangentially (it eventually cuts this line at T_D), due to the existence of a total wetting state at coexistence. Later, the nematic phase was confined by symmetric walls, i.e., both walls favored the same orientation (homeotropic) [10]. Then also the same anchoring line appeared, and it was found to be very insensitive to the pore width except with respect to the localization of T_D, which is shifted by capillary effects. These findings have a bearing on the phenomenology that appears when the liquid crystal is confined.

In the present paper, the theory is generalized to the case where the walls compete in molecular alignment. We believe that deeper insight into the surface-induced effects in liquid crystals can be obtained from a molecular approach and, in this respect, density-funtional theory appears to be a powerful tool. The confinement of the nematic phase is imposed by the presence of a boundary made up of two opposing flat surfaces, one favoring homeotropic orientation and the other favoring planar orientation. In these conditions, a spatial variation in the tilt angle between the director and the surface normal is found. The textures adopted by the nematic direc-

*Corresponding author. Electronic address: inma@likix2.us.es

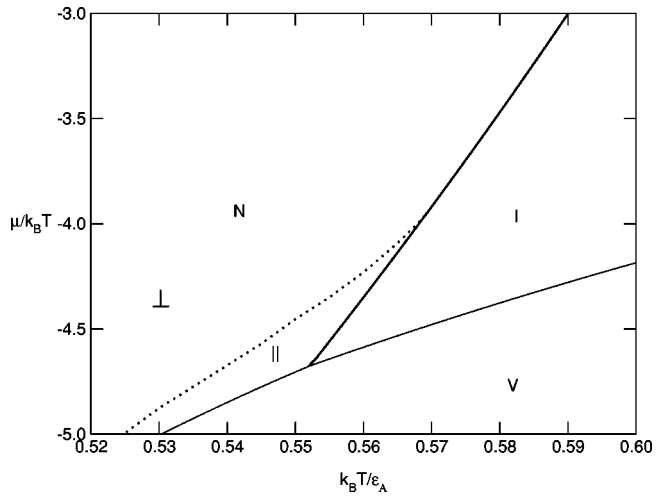

FIG. 1. Phase diagram containing bulk phase transitions and the anchoring transition for the case $\epsilon_W/\epsilon_A=0.53$ (they join at the temperature T_D). NI coexistence is denoted by the thick solid line. The dotted line is the anchoring line for the case of a nematic in the presence of a single surface that favors homeotropic orientation; this line divides the nematic phase into a region with homeotropic ($\perp$) and planar ($\parallel$) nematic states. The thin solid line corresponds to the bulk transitions involving the vapor phase.

tor depend very dramatically on the values of both surface field and pore width. For the case of a strong surface field ϵ_W and a wide pore this dependence is linear with respect to the coordinate normal to the interfaces except close to the surfaces. This configuration satisfies surface boundary conditions but entails an elastic energy which is a minimum for a linear tilt configuration. For weaker surface fields and/or narrow pores a different texture occurs where the tilt angle adopts a steplike configuration. Our calculations also reveal the existence of biaxial behavior close to the surface favoring planar orientation as well as in a small region associated with the change of orientation in the steplike configuration. These biaxilities are direct surface effects due to the existence of different interfaces.

In the next section we give a short account of the theoretical model used to describe the structure and thermodynamics of the confined liquid crystal. In Sec. III we show the different tilt configurations that result and argue that the phase transition between the linear-tilt and the steplike-tilt configurations can be related to the anchoring transition found in the semi-infinite problem. We also discuss how biaxiality is affected by the pore width. We end with a section of conclusions.

II. THE MODEL

The theoretical model is a standard generalized van der Waals theory based on a perturbative expansion, using a hard-sphere fluid as reference system [11]. Details of the physical basis of the model and how to obtain its solutions numerically can be found elsewhere [12,13]. Our starting point is the grand potential functional per unit system area A, $\Omega[\rho]/A$, whose functional minimum with respect to the one-particle distribution function $\rho(\mathbf{r},\hat{\mathbf{\Omega}})$, which depends on both molecular positions $\mathbf{r}$ and orientations $\hat{\mathbf{\Omega}}$, gives the equilibrium structure of the interface. This function $\rho(\mathbf{r},\hat{\mathbf{\Omega}}) \equiv \rho(z) f(z,\hat{\mathbf{\Omega}})$ contains a mass distribution $\rho(z)$ and an angular distribution $f(z,\hat{\mathbf{\Omega}})$. These quantities vary locally with the distance from $z=0$ to $z=H$, H being the pore width. The expression for $\Omega[\rho]$ in a mean field approximation is

$$\Omega[\rho]=F_r[\rho]+\frac{1}{2}\int\int\int\int d\mathbf{r}d\mathbf{r}'d\hat{\mathbf{\Omega}}d\hat{\mathbf{\Omega}}'\rho(\mathbf{r},\hat{\mathbf{\Omega}}) \times\rho(\mathbf{r}',\hat{\mathbf{\Omega}}')v(\mathbf{r}-\mathbf{r}',\hat{\mathbf{\Omega}},\hat{\mathbf{\Omega}}') -\int\int d\mathbf{r}d\hat{\mathbf{\Omega}}\rho(\mathbf{r},\hat{\mathbf{\Omega}})[\mu-v_W(\mathbf{r},\hat{\mathbf{\Omega}})], \quad (1)$$

where μ is the chemical potential and

$$F_r[\rho]=\int d\mathbf{r} f_{hs}(\rho(\mathbf{r}))+k_BT\int d\mathbf{r}\rho(\mathbf{r})\langle\ln[4\pi f(z,\hat{\mathbf{\Omega}})]\rangle$$

is the reference system free energy. In the above expression $f_{hs}(\rho(\mathbf{r}))$ is the hard-sphere free energy density of a uniform fluid with a density equal to the local density at $\mathbf{r}$ and $\langle\cdots\rangle$ is an angular average. The attractive potential v contains anisotropic (dispersion) forces driving the liquid-crystalline behavior of the model material:

$$v(\mathbf{r},\hat{\mathbf{\Omega}},\hat{\mathbf{\Omega}}')=v_A(r)+v_B(r)P_2(\hat{\mathbf{\Omega}}\cdot\hat{\mathbf{\Omega}}')+v_C(r)[P_2(\hat{\mathbf{\Omega}}\cdot\hat{\mathbf{r}}) +P_2(\hat{\mathbf{\Omega}}'\cdot\hat{\mathbf{r}})], \quad (2)$$

where $\hat{\mathbf{r}}=\mathbf{r}/r$, and $v_A(r)$, $v_B(r)$, and $v_C(r)$ are functions of the intermolecular center-of-mass distance r. Note that this potential is adequate to model uniaxial molecules with top-bottom symmetry. In this work we choose them to have a simple Yukawa form, i.e., $v_i(r)=-\epsilon_i\exp[-\lambda_i(r-\sigma)]/r$ for $r>\sigma$, and $v_i(r)=0$ otherwise, where σ is the diameter of the hard sphere.

The walls are modeled via the following potentials:

$$v_W^1(z,\theta)=-\epsilon_W e^{-\lambda_W(z-\sigma)}P_2(\cos\theta) \quad \text{(left wall, } z=0\text{)}, \quad (3)$$

which favors homeotropic anchoring, and

$$v_W^2(z,\theta)=\epsilon_W e^{-\lambda_W[-(z-H)-\sigma]}P_2(\cos\theta) \quad \text{(right wall, } z=H\text{)}, \quad (4)$$

which favors planar alignment. The parameter ϵ_W is the surface strength of the walls and plays an important role in anchoring phenomena.

In order to describe the orientational structure of the fluid a tensorial order parameter is defined as

$$Q_{\alpha\beta}=\int d\hat{\mathbf{\Omega}}f(z,\hat{\mathbf{\Omega}})\left(\frac{3\hat{\Omega}_\alpha\hat{\Omega}_\beta-\delta_{\alpha\beta}}{2}\right) \quad (5)$$

where $\delta_{\alpha\beta}$ is the Kronecker symbol and $\hat{\Omega}_\alpha$ is the α component of $\hat{\mathbf{\Omega}}$. This quantity is a traceless symmetric tensor with eigenvalues $\lambda_1 \geqslant \lambda_2 \geqslant \lambda_3$. In this description, the isotropic state is defined by the condition $\lambda_1=\lambda_2=\lambda_3=0$. Uniaxial states occur when there is a twofold degenerate eigenvalue and then two cases can be distinguished: the uniaxial nematic state ($\lambda_1>\lambda_2=\lambda_3$) and the random planar case ($\lambda_1=\lambda_2>\lambda_3$). In the first case, the molecules align preferentially along the director, defined as the eigenvector corresponding to the largest eigenvalue (the uniaxial order parameter $U \equiv \lambda_1$). In the second case, the molecular orientations are uniformly distributed on a plane perpendicular to the eigenvector corresponding to the lowest eigenvalue.

For the case of nondegenerate eigenvalues, we can define the uniaxial (U) and biaxial (B) order parameters in terms of the eigenvalues of this tensor. The former is defined, as before, as the largest eigenvalue of the order parameter tensor (λ_1) and the corresponding eigenvector is the local director of the fluid. The biaxial parameter is proportional to the difference of the two smallest eigenvalues. This quantity gives information on the amount of orientational order on the plane perpendicular to the director. In this way, a secondary director can be defined as the eigenvector corresponding to the eigenvalue λ_2. By the symmetry of the problem, we have focused on the case where the director varies in the x-z plane and is invariant with respect to a reflexion $y \to -y$. In these conditions, the director is characterized by the tilt angle ψ, defined as the angle formed between the director and the z axis. By convention, we define $B=\pm 2(\lambda_2-\lambda_3)/3$, with $B>0$ if the secondary director is on the x-z plane and $B<0$ if it is along the y axis.

For numerical reasons, it is convenient to obtain the orientation distribution of the molecules referred to a laboratory reference system, described by three order parameters,

$$\eta(z)=\int d\phi \sin\theta d\theta f(z,\hat{\mathbf{\Omega}}) P_2(\cos\theta), \tag{6}$$

$$\nu(z)=\int d\phi \sin\theta d\theta f(z,\hat{\mathbf{\Omega}}) \sin 2\theta \cos\phi, \tag{7}$$

$$\sigma(z)=\int d\phi \sin\theta d\theta f(z,\hat{\mathbf{\Omega}}) \sin^2\theta \cos 2\phi. \tag{8}$$

These independent parameters can be related to the set $\{\psi,U,B\}$ by the following expressions:

$$\tan\psi(z)=\frac{\nu(z)}{\eta(z)-\sigma(z)/2+\sqrt{[\eta(z)-\sigma(z)/2]^2+\nu(z)^2}}, \tag{9}$$

$$U(z)=\frac{1}{4}\left(\eta(z)+\frac{3}{2}\sigma(z) + 3\sqrt{[\eta(z)-(1/2)\sigma(z)]^2+\nu(z)^2}\right), \tag{10}$$

$$B(z)=\frac{1}{2}\left(\eta(z)+\frac{3}{2}\sigma(z)-\sqrt{[\eta(z)-(1/2)\sigma(z)]^2+\nu(z)^2}\right). \tag{11}$$

Numerical values for the potential parameters were taken as $\epsilon_A=1$ (which sets the temperature scale), $\epsilon_B/\epsilon_A=0.847$, and $\epsilon_C/\epsilon_A=0.75$. The range parameters λ_i are set, in units of σ (throughout we choose this unit to set the length scale), to $\lambda_i=2,4,1.75$ ($i=A,B,C$) and $\lambda_W=1$. The model predicts a bulk phase diagram with vapor, isotropic liquid, and nematic liquid coexisting at a triple point temperature T_{NIV} [11].

III. RESULTS

Confinement of simple liquids generally brings about capillary effects and associated capillary condensation phenomena whereby condensation occurs below the saturation point in bulk, as measured, for example, by the chemical potential. Similar phenomena must occur in nematic liquid crystals but with additional complicating factors due to the orientational order induced by the confining surfaces.

In the following we use the chemical potential μ as the external thermodynamic potential, in addition to the temperature T. Capillary condensation of the nematic from the isotropic phase occurs when, at fixed μ, the temperature $T_{NI}(H)$ at which the pore becomes filled with an oriented (nematic) phase is shifted with respect to the corresponding temperature in bulk $T_{NI}(\infty)$. We are thus seeking a nonzero value of $\Delta T \equiv T_{NI}(H)-T_{NI}(\infty)$. Our calculations reveal that, contrary to the case of symmetric walls [10], for large pore widths (H larger than 20σ) no significant capillary effect exists, i.e., we find that the nematic-isotropic transition occurs at the same temperatures as in the bulk state. However, there are indications that for smaller pore widths this situation is no longer true (this aspect is currently being studied). Note though that condensation lines involving confined vapor states are expected to be affected by confinement; since these lines are not central to our argument we do not give any results in the following.

Figure 1 shows the bulk phase diagram, with vapor (V), isotropic (I), and nematic (N) phases and their corresponding phase transitions. We have superimposed the anchoring line, representing surface phase transitions between states with different director alignments for the semi-infinite problem (i.e., only one surface, inducing homeotropic alignment). The states localized to the right of the anchoring line possess homeotropic alignment and the states localized to the left possess planar alignment. These results were obtained with a surface field $\epsilon_W/\epsilon_A=0.53$; for larger values this transition curve tends to approach the coexistence lines, reducing the region of planar states [9].

Next we calculated equilibrium states but with the sample confined between two opposing walls separated by a distance H. There is a molecular ordering field due to the surfaces through the potential parameter ϵ_W. If the surface field strength is sufficiently high, one expects the director to adopt the configuration that satisfies the orientation favored by each surface, at least approximately. However, this necessarily demands that the director becomes distorted within the

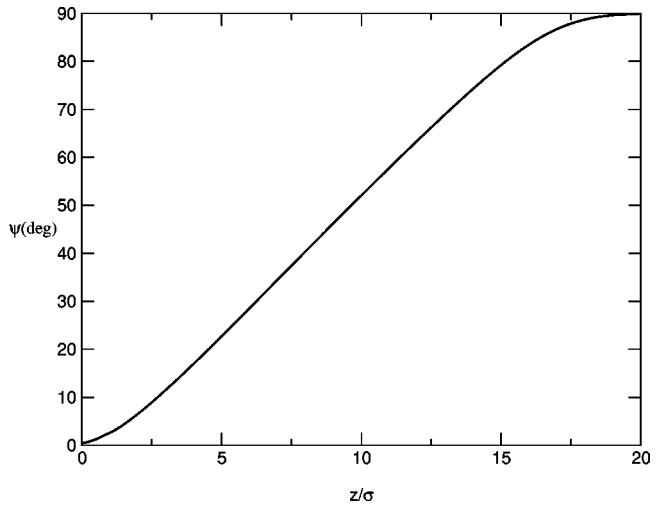

FIG. 2. Tilt-angle profile for a confined nematic at $k_BT/\epsilon_A = 0.57$ and $\mu/k_BT = -3.7$ (L phase). Values for the surface field and pore width are $\epsilon_W/\epsilon_A = 0.7$ and $H = 20\sigma$, respectively.

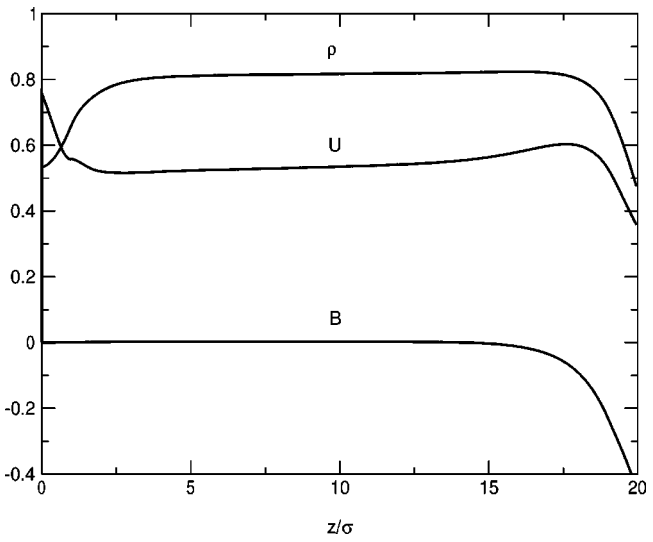

FIG. 3. Density (ρ) and uniaxial (U) and biaxial (B) order parameter profiles for the L phase. $\epsilon_W/\epsilon_A = 0.7$ and values of T and μ are given in text.

pore, which entails a free energy cost due to the elastic contribution. In fact, the distribution of this inhomogeneity along the pore is found to depend sensitively on the values of pore width and surface field strength, and is expected to depend also on the thermodynamic parameters μ and T.

Competition between these two energies results in the existence of two tilt configurations: L, where the tilt angle rotates uniformly along the pore and the resulting tilt-angle profile is linear in z; S, where the tilt angle adopts a steplike configuration, being constant throughout the sample except in a narrow region close to the $z = 0$ surface where a crossover exists from 0° (homeotropic) to 90° (planar). This variation in the tilt-angle profile has also been described by Žarlah and Žumer employing a semiphenomenological approach for the study of a confined nematic film [20].

Figure 2 shows an L phase for $H = 20\sigma$, $\epsilon_W/\epsilon_A = 0.7$, and for thermodynamic conditions of temperature and chemical potential where, in the semi-infinite case, the nematic is clearly in the homeotropic state ($\mu/k_BT = -3.7, k_BT/\epsilon_A = 0.57$). In the middle of the pore the tilt profile is almost a linear function of z, approaching smoothly the favored values at the walls.

In Fig. 3 the density and the uniaxial and biaxial order parameter profiles are plotted for the L phase. The profiles present a smooth behavior, reaching a clear plateau in the middle of the pore with values close to the bulk values. The vanishing value of B in regions far from the interfaces is consistent with the uniaxial nature of the fluid particles. Close to the walls the profile behaves differently depending on the favored orientation. Around the $z = 0$ surface the U order parameter increases due to the strong surface interaction (despite a decay in density). However, these deformations do not induce biaxiality (i.e., $B = 0$) due to the smooth character of the tilt profile along the pore. On the other hand, near the $z = H$ surface, where the tilt angle is 90°, the U order parameter gets lower values and $B < 0$, which reflects the orientation of the molecules mainly distributed on the x-y plane, the x axis being the in-plane preferred direction (director) and with some small degree of order along the y axis (secondary director). The decrease of the amount of order is due to the surface potential which promotes a random planar distribution.

If the surface field strength is reduced the director tilt configuration changes to a step, i.e., an S phase. Here the tilt angle is uniform and equal to 90° except in a narrow homeotropic region close to the homeotropic wall (Fig. 4). In general, this homeotropic region increases with increasing wall-particle potential range and with increasing strength of the surface field, so for the case of $\epsilon_W/\epsilon_A = 0$ one recovers the configuration that corresponds to a nematic–hard-wall interface (planar throughout the pore). Note that the S phase is spatially asymmetric, the tilt orientation being different from planar only in a small region close to the homeotropic wall. In fact, a corresponding S phase where the tilt was in a ho-

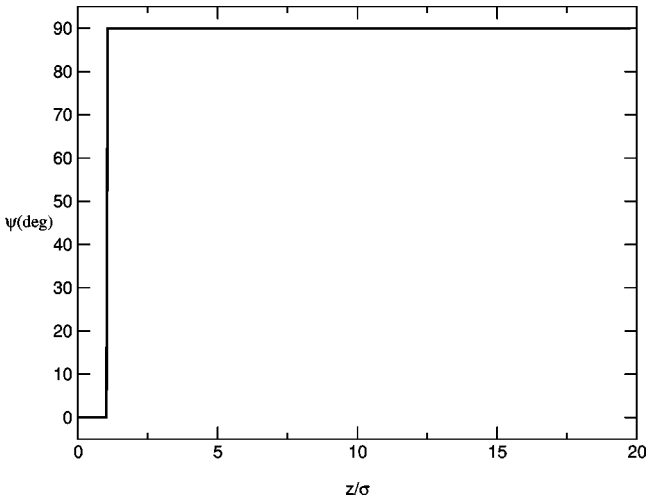

FIG. 4. Tilt-angle profile for a confined nematic with surface field $\epsilon_W/\epsilon_A = 0.30$ (S phase). The values of T, μ, and H are the same as in Fig. 2.

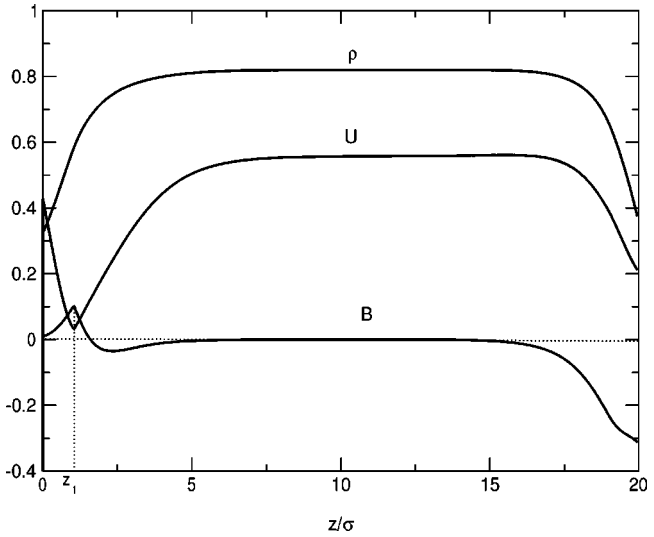

FIG. 5. Density (ρ) and uniaxial (U) and biaxial (B) order parameter profiles for the S phase. $\epsilon_W/\epsilon_A=0.3$ and the values of T and μ are the same as in Fig. 2.

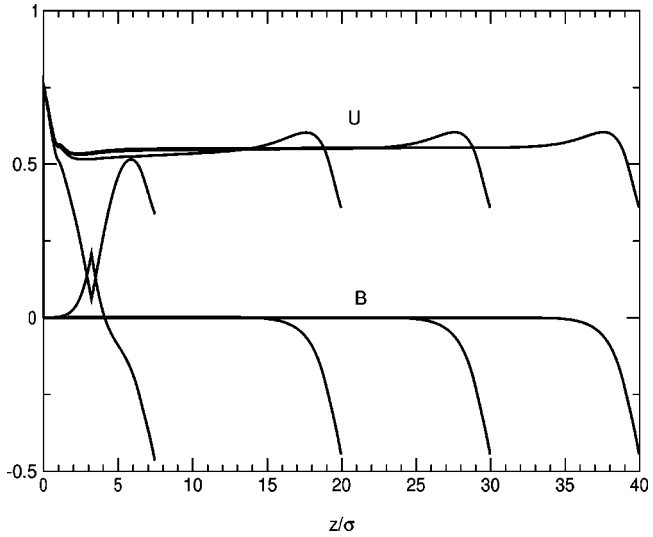

FIG. 6. Uniaxial (U) and biaxial (B) order parameter profiles for different pore widths and $\epsilon_W/\epsilon_A=0.7$. The pore widths H are, from left to right, 7.5σ, 20σ, 30σ, and 40σ. The values of T and μ are the same as in Fig. 2.

meotropic configuration except in a very small region close to the planar wall is not observed in our calculations because of the effect due to the ordering field acting through the potential parameter ϵ_C. This field promotes molecular configurations where the director lies along a direction either perpendicular or parallel to the direction of inhomogeneity, depending on the sign of ϵ_C ($\epsilon_C>0$ or $\epsilon_C<0$, respectively). In our case $\epsilon_C>0$, which means that the preferred director orientation is planar except in the region, close to $z=0$, where the effect of the wall promoting homeotropic alignment is more pronounced.

In Fig. 5 we plot the density and uniaxial and biaxial order parameter profiles in the S phase obtained with $\epsilon_W/\epsilon_A=0.30$. Again, the profiles deviate from the bulk values only close to the surfaces. The deviation around $z=H$ has the same origin as that in the L phase. However, close to $z=0$ this behavior has a different nature. An analysis of the order parameter profiles reveals that the system goes *smoothly* from a homeotropic to a planar configuration via a random planar state in the x-z plane. This point (z_1 in Fig. 5) corresponds to a jump of the tilt (origin of the step function profile). This mechanism is reponsible for the decay of the order and the biaxial behavior around this region. In fact, the existence of a crossover between a homeotropic configuration and a planar configuration is closely linked to the capability of the fluid to have biaxial behavior in a small spatial range between the two anchoring states. So the roles that the z and x axes play as the local director and secondary director, respectively, for $0<z<z_1$ are exchanged at $z=z_1$. However, in order to make this mechanism feasible a dramatic depletion of the amount of order is needed. Moreover, the secondary director changes its alignment from the z axis to the y axis as z is increased (i.e., B changes its sign), before the biaxiality virtually disappears in the middle of the pore. Biaxiality directly induced by the breaking of symmetry associated with the presence of the interfaces and in the case of a free interface with planar director alignment has been observed in simulations [14].

In order to study in more detail the dependence of the nematic ordering on the pore width, we have calculated uniaxial order and biaxiality profiles for different values of H and for $\epsilon_W/\epsilon_A=0.7$ (Fig. 6). For pore widths $H=20\sigma,30\sigma$, and 40σ, for which the L phase is the stable phase, the profiles exhibit inhomogeneity regions close to the surface favoring planar alignment, being almost constant in the rest of the pore. Note that biaxiality occurs only where the tilt angle is significantly close to 90°. An interesting feature is that the order parameter profiles converge around $z=0$ ($z=H$) to the profiles obtained for the $z=0$ surface against a nematic in a homeotropic configuration (the $z=H$ surface against a nematic in a planar configuration). Furthermore, such semi-infinite profiles are the equilibrium ones for these values of ϵ_W, μ, and T. On the other hand, for $H=7.5\sigma$, the stable phase is the S phase, and additional regions of inhomogeneity (and biaxiality) develop in the neighborhood of the $z=0$ surface.

The transition between the L and S phases involves a finite free energy barrier, implying the existence of a thermodynamic first-order phase transition between the two phases. This is revealed by computing the relevant free energy for confined systems, i.e., the grand potential, as a function of the potential parameters and/or the thermodynamic parameters μ and T. In our case we have chosen to fix the latter and vary ϵ_W. Figure 7 shows the behavior of the grand potential as a function of ϵ_W. Two branches, corresponding to the L and S phases, are shown. The point where the branches cross, ϵ_W^c, gives the transition point. Note the existence of metastable branches in both phases, which indicates the first-order nature of the phase transition. Tilt-angle profiles along the pore corresponding to the coexisting L and S phases at $\epsilon_W/\epsilon_A=\epsilon_W^c/\epsilon_A=0.554$ for $H=20\sigma$ are shown in Fig. 8. Note that the linear behavior in the L phase has a smaller

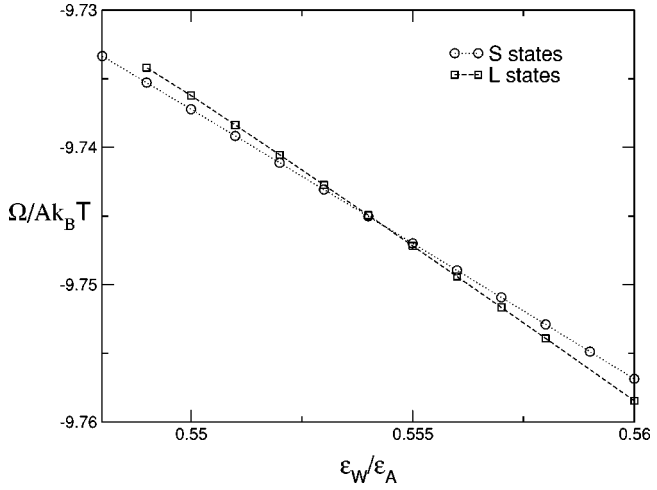

FIG. 7. Thermodynamic grand potential as a function of the surface field ϵ_W for thermodynamic conditions and pore width as in Fig. 2. Branches corresponding to steplike (S) and linear (L) tilt-angle profiles are shown. The point at which these branches cross gives the transition point at $\epsilon_W^c/\epsilon_A = 0.554$. The values of T, μ, and H are the same as in Fig. 2.

range and its slope is also less than in the case presented in Fig. 2. On the other hand, the step in the S phase is located further from the $z=0$ surface than in the case presented in Fig. 4.

As in any analysis of metastable states, some caution has to be exercised in analyzing the occurrence of the different phases. In particular, the initial conditions required in our numerical minimization scheme have to be chosen carefully. For example, the reality of the metastable L branch is shown by performing the following analysis: (i) Equilibrium S states at low ϵ_W are obtained by conducting minimization processes starting from linear and steplike profiles; these processes give the same equilibrium S states. (ii) For higher, increasing values of ϵ_W, using steplike profiles or linear profiles as starting conditions give different final states beyond

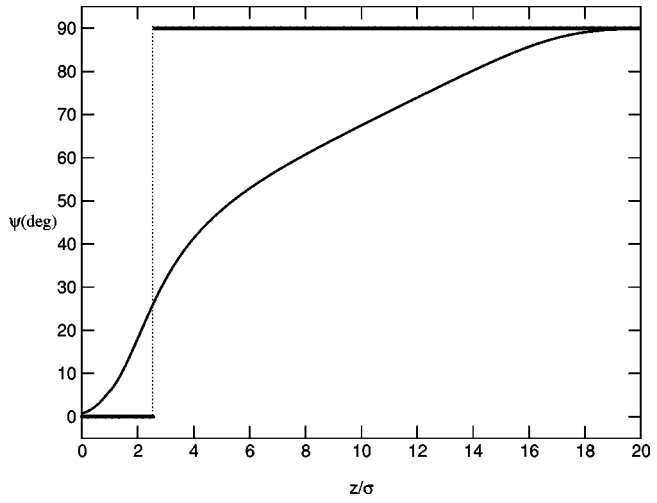

FIG. 8. Tilt-angle profiles for L and S phases at coexistence corresponding to pore width $H=20\sigma$ and critical value $\epsilon_W^c/\epsilon_A = 0.554$. The values of T and μ are the same as in Fig. 2.

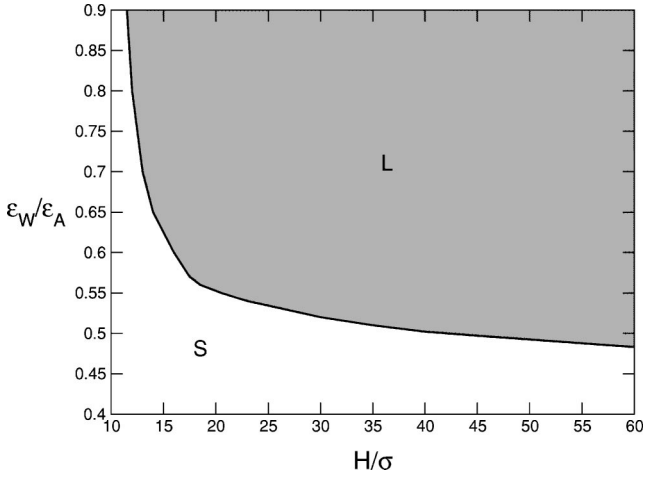

FIG. 9. Phase diagram in the ϵ_W-H plane. The values of T and μ are the same as in Fig. 2.

the transition point ϵ_W^c, the final L states having lower grand potential energies than the final S states. This is the region of metastability of the S phase. Proceeding in the same way but from the L branch at high ϵ_W and decreasing ϵ_W provides the metastability region for the L phase.

Figure 9 shows the global phase diagram with respect to the parameters ϵ_W and H and for thermodynamic conditions $T=0.57$ and $\mu=-3.7$. The line indicates the phase transition separating L and S phases. As the pore width is increased, the region of stability of the L phase is enlarged since the elastic energy associated with the deformation of the director along the pore (proportional to the integrated squared gradient of the tilt profile) decreases, as opposed to the case of the S phase, for which this energy is essentially constant and seems to approach asymptotically the value of $\epsilon_W=\epsilon_W^a$, at which the anchoring transition occurs for the semi-infinite case of the nematic against the $z=0$ wall. For narrow pores, we find a quick increase of ϵ_W^c as the pore width is reduced, indicating that, in order for the L phase to become stable, a large surface field is required to compensate for the large elastic energy associated with a high tilt-angle gradient. An interesting issue, which we have been unable to address for technical reasons, is whether this first-order phase transition may end up at a critical point as the pore width is reduced or even become second order through the appearance of a tricritical point.

An analysis of the results quoted above shows that there is a relationship between the L-S transition and the anchoring transition observed in the semi-infinite problem. Let us consider the case of $H \gg \sigma$. We have observed that the density and order parameter profiles deviate from the bulk values only in regions around the surfaces that are the ranges of the inhomogeneities of the order of the molecular interactions. This feature is not surprising for the S phase, since in the middle of the pore the nematic is in a nondistorted tilt configuration (i.e., planar), so its tilt profile can be understood as two uncorrelated semi-infinite profiles linked via the bulk planar state. However, this fact is also true for the L phase even when the tilt distortion is propagated through the pore (see the discussion of Fig. 6 above). This is the scenario that

the phenomenological theory implicitly assumes: The excess free energy $\Delta\Omega=\Omega+pV$ (where p is the bulk pressure and $V=AH$ is the volume of the sample) can be split into two terms, an elastic term $\Delta\Omega^e$ that comes from the distortions of the director field on a macroscopic scale, and surface terms $\Delta\Omega^{surf}_{z=0}$ and $\Delta\Omega^{surf}_{z=H}$ that include the effect of the density and order parameter inhomogeneities on a microscopic scale close to the boundaries. The elastic term is given in terms of the elastic constants K_1, K_2, K_3, and K_{24} by the Oseen-Frank free energy [15,16] as

$$\Delta\Omega^e=\frac{K_1}{2}(\boldsymbol{\nabla}\cdot\mathbf{n})^2+\frac{K_2}{2}(\mathbf{n}\cdot\boldsymbol{\nabla}\times\mathbf{n})^2+\frac{K_3}{2}(\mathbf{n}\times\boldsymbol{\nabla}\times\mathbf{n})^2 -(K_2+K_{24})\boldsymbol{\nabla}\cdot(\mathbf{n}\boldsymbol{\nabla}\cdot\mathbf{n}+\mathbf{n}\times\boldsymbol{\nabla}\times\mathbf{n}) \tag{12}$$

where $\mathbf{n}(\mathbf{r})$ is the director field. Note that the splay-bend term is not included since $K_{13}=0$ in bulk [17]. If we restrict our study to the cases in which there is translational symmetry in the x-y plane and the director is assumed to be in the x-z plane (there is no twist), then $\mathbf{n}(\mathbf{r})=(\cos[\psi(z)],0,\sin[\psi(z)])$. In our model of uniaxial molecules with top-bottom symmetry, $K_1=K_3=-2\pi\rho_b^2U_b^2\int_0^\infty dr r^4 v_B(r)$, where ρ_b and U_b are the bulk density and uniaxial order parameter, respectively [19,17]. So the total excess free energy is given by

$$\frac{\Delta\Omega}{A}=\frac{\Delta\Omega^{surf}_{z=0}(\psi(0),\psi'(0))}{A}+\frac{\Delta\Omega^{surf}_{z=H}(\psi(H),\psi'(H))}{A} +\frac{K_3}{2}\int_0^H dz[\psi'(z)]^2 \tag{13}$$

where $\psi'\equiv d\psi/dz$. Note the dependence of the surface terms on the contact values at the boundaries of the tilt angle and its derivative with respect to z [18]. Functional minimization of Eq. (13) leads to an equilibrium tilt linear profile $\psi'=\text{const}=O(1/H)$. The exact expression for the profile will depend on the surface terms of the free energy, so some information about them is needed. The values of $\Delta\Omega^{surf}_{z=0}$ can be obtained microscopically from the excess free energy corresponding to the case of a wall against a distorted nematic whose tilt profile varies asymptotically as $\psi(0)+\psi'(0)z$ for $\sigma\ll z\ll H$ (this discussion is analogous for the $z=H$ case). Since $\psi'(0)\ll 1/\sigma$ the effect of the distortion far from the $z=0$ surface will be a perturbation with respect to the case $\psi'=0$, which corresponds to the semi-infinite case studied in [9]. In this reference it was shown that, if the wall promotes homeotropic anchoring, depending on the ratio between ϵ_W and ϵ_C two local minima can appear for $\psi=0°$ and $\psi=90°$ (S phase) with a free energy barrier between them. However, if the surface favors planar anchoring only a global minimum at $\psi=90°$ can exist. We can now expand the surface free energy in a series of both ψ and ψ' around $(\psi,\psi')=(0°,0)$ and $(90°,0)$. The special symmetry of our problem (rotational invariance around the z axis and the top-bottom symmetry of the molecules) implies that the linear term in ψ' vanishes. From this analysis we can conclude that for $H\gg\sigma$ two different states can exist: a linear state that goes from a tilt close to 0° at $z=0$ to a value close to 90° at $z=H$, and a state with nondistorted planar tilt through the pore. The former corresponds to the L phase described with the microscopic approach and the latter corresponds to the S phase on the scale defined by H, and where the inhomogeneities *on the microscopic scale* are localized around the walls. These states correspond to the L and S phases described by the microscopic approach. For the latter, a remark is needed. A direct application of the phenomenological functional to the sharp step profile in the tilt angle would lead to a divergence on the free energy due to an elastic contribution. However, we have seen that the step associated with the inhomogeneities of the intrinsic order parameter profiles and consequently the elastic free energy is inadequate to describe the step. This is the reason that a surface term is needed to account for the step ($\Delta\Omega^{surf}_{z=0}$).

Furthermore, by using this phenomenological approach a first-order transition can be predicted close to the anchoring line, inside the homeotropic region. Equation (13), up to terms of the order of $O(1/H)$, is

$$\frac{\Delta\Omega}{A}=\frac{\Delta\Omega^{surf}_{z=0}(\psi_0,0)}{A}+\frac{\Delta\Omega^{surf}_{z=H}(\pi/2,0)}{A}+\frac{K_3}{2H}\left(\frac{\pi}{2}-\psi_0\right)^2 \tag{14}$$

where $\psi_0=0$ or $\pi/2$ for the L and S states, respectively. The transition occurs for

$$H_t=\frac{\pi^2K_3}{8[\Delta\Omega^{surf}_{z=0}(\pi/2,0)-\Delta\Omega^{surf}_{z=0}(0,0)]} \tag{15}$$

which implies that $\Delta\Omega^{surf}_{z=0}(\pi/2,0)>\Delta\Omega^{surf}_{z=0}(0,0)$, i.e., the conditions should correspond to having a homeotropic configuration in the semi-infinite case, and the transition is first order due to the free energy barrier that exists between the two minima for the semi-infinite case. So, for $H>H_t$ a stable L configuration exists and for $H<H_t$ the S state is the stable one. From Eq. (15) it is clear that $H_t\to\infty$ as the system approaches the anchoring line [characterized by the condition $\Delta\Omega^{surf}_{z=0}(\pi/2,0)=\Delta\Omega^{surf}_{z=0}(0,0)$], i.e., the L-S transition occurs for infinitely wide pores and, consequently, the anchoring line can be understood as the limit of the L-S transition for $H\to\infty$.

Strictly speaking, the scenario presented above is true only for $H\gg\sigma$. However, our calculations reveal that the L-S transition observed by our density-functional theory (DFT) calculations is the continuation of the transition predicted for wide pores. First of all, the free energy of the S phase is expected to converge toward its limiting value given by Eq. (14) very fast, as was observed in the symmetric walls case in [10]. For the L phase, we have compared the DFT results for $\epsilon_W/\epsilon_A=0.7$ with the limiting expression given by Eq. (14) (see Fig. 10). The values of μ and T are the same as in all our calculations, i.e., $\mu/k_BT=-3.7$ and $k_BT/\epsilon_A=0.57$. For such conditions, $K_3\sigma/\epsilon_A=0.615$. On the other hand, calculations for the semi-infinite case show that the asymptotic value for $H\to\infty$ is given by $\Delta\Omega/Ak_BT=1.841$. It is clear that the values of $\Delta\Omega$ converge for relatively small values of

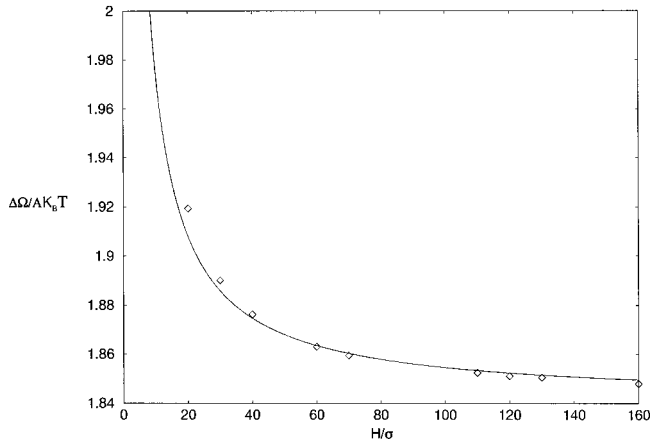

FIG. 10. Comparison between the density-functional theory and the phenomenological theory (expression in the text). The diamonds correspond to the excess free energy per area in units of k_BT of a nematic confined by opposing walls in the L state with $k_BT/\epsilon_A = 0.57$, $\mu/k_BT = -3.7$, and $\epsilon_W/\epsilon_A = 0.7$, calculated by using the density-functional approach. The solid line is the surface tension given by the phenomenological theory of Eq. (14).

H to the expression given by the phenomenological theory, and in any case the behavior is qualitatively correct. From this analysis we conclude that the L-S transition is driven by the anchoring (surface) transition that occurs for the semi-infinite case of a nematic against the $z=0$ surface.

IV. CONCLUSIONS

In this paper we have employed a well-tested generalized van der Waals theory to investigate the effect of confinement on the thermodynamics and microscopic structure of a nematic liquid crystal. The presence of two confining surfaces favoring opposite orientations of the nematic director makes the order parameter, which is a tensorial quantity, exhibit all of its richness, giving rise to capillary effects not present in simple, nonorientable fluids. The competing conditions at the surfaces imply a deformed state of the director inside the pore.

The main result of our study is that the system may adopt two possible states: one where the director changes orientation at an interface located close to the surface that favors homeotropic anchoring (depending on the wall-particle potential range), and one where the deformation takes place uniformly, giving rise to a basically linear tilt profile, with some degree of deformation close to the surfaces. The director may change from one configuration to the other via a first-order phase transition. The interplay between these two phases may be understood in terms of the competition between the elastic energy associated with a deformed director state and the energy associated with the orienting surfaces. We have also shown that this transition is closely linked with the planar-homeotropic transition observed in the semi-infinite problem. In order to prove this aspect, a phenomenological treatment has been employed. On the one hand, the theory shows how for big pores ($H \gg \sigma$) the L-S first-order transition can occur at a threshold value of the pore width H_t. On the other hand, the phenomenological approach also reveals that for $H \to \infty$ the L-S transition corresponds to the anchoring transition of the semi-infinite problem. We also conclude that the transition obtained by the DFT is the continuation to shorter scales of the transition predicted by the phenomenological theory, which in principle is valid only for much larger pore widths.

ACKNOWLEDGMENTS

I.R.P. would like to thank Professor R. Netz for his hospitality at LMU, which helped to develop this work. This research was supported by Grants No. PB97-0712 from DGICyT of Spain and No. FQM-205 from PAI of the Junta de Andalucía.

[1] J. Nehring and A. Saupe, J. Chem. Phys. **56**, 5527 (1972).
[2] G. Barbero, N.V. Madhusudana, and C. Oldano, J. Phys. (France) **50**, 2263 (1989).
[3] G. Skačej, A.L. Alexe-Ionescu, G. Barbero, and S. Žumer, Phys. Rev. E **57**, 1780 (1998).
[4] A. Poniewierski and A. Samborski, Liq. Cryst. **27**, 1285 (2000).
[5] J. Quintana and A. Robledo, Physica A **248**, 28 (1998).
[6] A.K. Sen and D.E. Sullivan, Phys. Rev. A **35**, 1391 (1987).
[7] R. van Roij, M. Dijkstra, and R. Evans, Europhys. Lett. **49**, 350 (2000).
[8] P.I.C. Teixeira, Phys. Rev. E **55**, 2876 (1997).
[9] I. Rodríguez-Ponce, J.M. Romero-Enrique, E. Velasco, L. Mederos, and L.F. Rull, Phys. Rev. Lett. **82**, 2697 (1999).
[10] I. Rodríguez-Ponce, J.M. Romero-Enrique, E. Velasco, L. Mederos, and L.F. Rull, J. Phys.: Condens. Matter **12**, A367 (2000).
[11] M.M. Telo da Gama, P. Tarazona, M.P. Allen, and R. Evans, Mol. Phys. **71**, 801 (1990).
[12] F.N. Braun, T.J. Sluckin, E. Velasco, and L. Mederos, Phys. Rev. E **53**, 706 (1996); An alternative numerical approach is that used by E. Martín del Río, M.M. Telo da Gama, E. de Miguel, and L. Rull, *ibid.* **52**, 5028 (1995).
[13] Y. Martínez, E. Velasco, A.M. Somoza, L. Mederos, and T.J. Sluckin, J. Chem. Phys. **108**, 2583 (1998).
[14] G.D. Wall and D.J. Cleaver, Phys. Rev. E **56**, 4306 (1997).
[15] C.W. Oseen, Trans. Faraday Soc. **29**, 833 (1933).
[16] F.C. Frank, Discuss. Faraday Soc. **25**, 19 (1958).
[17] H. Yokoyama, Phys. Rev. E **55**, 2938 (1997).
[18] M. Faetti and S. Faetti, Phys. Rev. E **57**, 6741 (1998).
[19] P.I.C. Teixeira, J. Chem. Phys. **97**, 1498 (1992).
[20] A. Šarlah and S.S. Žumer, Phys. Rev. E **60**, 1821 (1999).